Recellularization of bronchial extracellular matrix with primary bronchial smooth muscle cells

Selma Ben Hamouda[1]*, Amandine Vargas[1], Roxane Boivin[1], Maria Angelica Miglino[2], Renata Kelly da Palma[3], Jean-Pierre Lavoie[1]*.

[1] Department of Clinical Sciences, Faculty of Veterinary Medicine, University of Montreal, St-Hyacinthe, Quebec, Canada

[2] School of Veterinary Medicine and Animal Sciences, University of Sao Paulo, São Paulo, Brazil

[3] Institute for Bioengineering of Catalonia, Barcelona, Spain

* Corresponding authors:

Jean-pierre.lavoie@umontreal.ca (JPL)

Selma.ben.hamouda@umontreal.ca (SBH)

Abstract

Severe asthma is associated with an increased airway smooth muscle (ASM) mass and an altered composition of the extracellular matrix (ECM). Studies have indicated that ECM-ASM cell interactions contribute to this remodeling and its limited reversibility with current therapy. Three-dimensional matrices allow the study of complex cellular responses to different stimuli in an almost natural environment. Our goal was to obtain acellular bronchial matrices and then develop a recellularization protocol with ASM cells. We studied equine bronchi as horses spontaneously develop a human asthma-like disease. The bronchi were decellularized using Triton/Sodium Deoxycholate. The obtained scaffolds retained their anatomical and histological properties. Using immunohistochemistry and a semi-quantitative score to compare native bronchi to scaffolds revealed no significant variation for matrixial proteins. A DNA quantification and electrophoresis indicated that most of DNA was 29.6 ng/mg of tissue ± 5.6 with remaining fragments of less than 100 bp. Primary ASM cells were seeded on the scaffolds. Histological analysis after recellularization showed that ASM cells migrated and proliferated primarily in the decellularized smooth muscle matrix, suggesting a chemotactic effect of the scaffolds. This is the first report of primary ASM cells preferentially repopulating the smooth muscle matrix layer in bronchial matrices. This protocol is now being used to study the molecular interactions occurring between the asthmatic ECMs and ASM to identify effectors of asthmatic bronchial remodeling.

Keywords: Decellularization, recellularization, airway smooth muscle cells, extracellular matrix, asthma.

Introduction

Asthma is a progressive and multi-component respiratory syndrome. Remodeling of the airways in asthma is characterized by structural changes leading to a thickening of the bronchial wall, airflow obstruction, and hyperreactivity of the airways [1]. In human asthma, tissue remodeling is believed to be only partially reversible or even irreversible following conventional treatments (corticosteroids / bronchodilators) even during extended periods of remission [2]. While airway remodeling is considered a target for asthma, little is known of the mechanisms involved in its development and reversibility. This is due to ethical considerations related to the invasiveness when sampling the airways, and technical limitations of the current imaging techniques.

As compared to single-layer culture, three-dimensional (3D) cell culture improves different cellular parameters including viability, adhesion, proliferation, etc. A study comparing the culture of skin fibroblasts on natural 3D matrices to their monolayer culture on different substrates revealed significant variations. Cell adhesion was 5 to 6 times greater on 3D matrix than on single-layer culture, cell migration was also increased and the acquisition of a morphology mimicking the in vivo appearance of the cells occurred faster [3]. A study of human embryonic stem cell differentiation found that cells were physiologically and morphologically more representative of the native cells when cultured on a 3D matrix than when cultured on flasks [4]. This is also supported by the finding that pulmonary fibroblasts response to tumor necrosis factor (TNF)α was increased in 3D culture when compared to monolayer culture [5]. There are different types of 3D culture including: 1) in suspension, 2) in gel scaffold or, 3) in natural or synthetic fibrous scaffold [6, 7]. Culturing cells on 3D bases is more difficult and

requires longer culture time than in monolayer, but the results obtained are believed to be more representative of the natural environment [6]. Thus, in order to evaluate the behavior of airway smooth muscle (ASM) cells in the asthmatic airways, we aimed to decellularize an equine respiratory bronchus while maintaining its architecture and protein composition to allow recellularization by bronchial smooth muscle cells. Equine bronchi were studied as horses spontaneously develop an asthma-like condition that shares clinical and remodeling features with human asthma [8]. Furthermore, it was shown in this model that the quantity of ASM is increased, and only partially reversible even after 1 year of inhaled corticosteroids [9, 10]. Results of the present study suggest that the bronchial smooth muscle cells preferentially colonize the bronchial smooth muscle extracellular matrix. These findings may allow investigating the interactions between smooth muscle cells and the extracellular matrix in the asthmatic airways.

Material and methods

Animals

Archived lung tissues from four asthmatic and three healthy control horses (5 mares and 2 geldings) aged 10-12 years from a tissue bank (htttp://www.btre.com) were studied. Four additional lungs were obtained from a slaughterhouse. The experimental protocol was approved by the ethical committee of the University of Montreal number Rech-1578.

Bronchi decellularization

Bronchi from 2nd to 4th generation were dissected from the surrounding lung tissues within 2 hours after euthanasia. The bronchi were then snap frozen in liquid nitrogen and

86 kept at -80°C until used. These bronchi were thaw and decellularized using a protocol
87 previously described [11] with minor modifications. Briefly, two consecutive cycles of
88 detergent (Triton 1X, Sodium deoxycholate and sodium chloride) and enzymatic (DNase)
89 treatments were followed by sterilization with paracetic acid-ethanol under continued
90 agitation to ensure the elimination of any immunogenic cellular material that may hinder
91 recellularization. Sections of bronchi were then paraffin-embedded for histology or snap
92 frozen for DNA and protein isolation.

93 Airway smooth muscle cell isolation and culture

94 Airway smooth muscle (ASM) cells were isolated from the same horses in the first hour
95 after the death, as previously described [12]. In brief, the ASM layer was collected from
96 the first bronchial bifurcation and then immersed in a digestion medium (Dulbeco's
97 Modified Eagle Medium / F12 nutrient mix (Thermofisher, Waltham, MA) with 0.125
98 U/ml Collagenase H (Sigma Aldrich, St. Louis, MO), 1 mg/ml Trypsin inhibitor (Sigma
99 Aldrich, St. Louis, MO), 1 U/ml elastase (Worthington biochemical, Lakewood, NJ), 1%
100 Penicillin-Streptomycin (Wisent Inc., Saint-Jean-Baptiste, QC) and 0.1% Fungizone
101 (Fisher Scientific, Hampton, NH)).

102 Cells (ASM) were seeded into ventilated cell culture flasks at 300,000 cells/cm^2 in
103 DMEM/F12 medium supplemented with 0.0024 mg/ml adenine, 10% non-
104 decomplemented fetal bovine serum (FBS) (Wisent Inc., Saint-Jean-Baptiste, QC), 1%
105 Penicillin-Streptomycin and 0.1% Fungizone and cultured at 37°C and 5% CO_2 for 48
106 hours. Media was then changed every 48 hours until confluence was reached. Cells were
107 frozen between the first and 4th passage (P) in liquid nitrogen until being used.

108 ## Smooth muscle cells characterization

109 ASM cells were characterized by flow cytometry before recellularization, as previously
110 described [12]. Briefly, cells were stained for intracellular markers with anti–α-SMA
111 (mouse IgG2a, Sigma Aldrich, St. Louis, MO, 1/250), anti-desmin (rabbit polyclonal
112 IgG, Abcam, Cambridge, UK, 1/200) and anti-SMMHC (rabbit IgG, Biomedial
113 technologies, Stoughton, MA, 1/300) antibodies for 1 hour. Cells were then washed 3
114 times and incubated for 30 minutes in the dark with fluorescent dye–conjugated anti-IgG
115 antibodies. Isotype-matched control antibodies (mouse IgG2a and rabbit IgG) were used
116 as negative control. All signals greater than those of the isotype-matched control
117 antibodies were considered positive, and degree of staining was evaluated as the mean
118 fluorescence intensity and mean percentage of positive cells. This characterization
119 showed simultaneous expression of α-SMA (mean±SEM) for 90% ± 8.6 cells, SMMHC
120 for 71% ± 16 cells and desmin for 85 ± 9.2 cells.

121 ## Assessment of decellularization efficiency

122 Decellularized bronchi were stained and compared to native bronchi using the Russel
123 modification of Movat Pentachrome [13]. The protocol was modified as the exposure
124 time to ferric chloride and to alcoholic safran solution was changed to 1 and 5 minutes,
125 respectively. Images were obtained at 100 and 200 magnifications using Panoptiq
126 software (version 2) connected to a Prosilica GT camera (model: GT1920C) mounted on
127 a Leica DM4000 B microscope.

128 DNA was isolated from 10 mg of frozen native and from freshly decellularized bronchi
129 using DNeasy blood and tissue Kit® (Invitrogen, Hilden, DE) as recommended by the

130 manufacturer. DNA was then visualized on agarose gel. Quantification of double-
131 stranded DNA before and after decellularization was done using the Qubit DNA BR
132 Assay kit (Invitrogen, Carlsbad, CA) according to the manufacturer instructions. Proteins
133 were extracted using T-PER (Thermofisher, Waltham, MA) and quantified using Qubit
134 Protein Assay Kit (Invitrogen, Carlsbad, CA).

135 Immunohistochemical staining for collagen I, collagen IV and fibronectin was performed
136 on 10% formalin preserved native and decellularized bronchi. Tissues were incubated
137 overnight with primary antibodies (collagen I; rabbit anti-bovine IgG, Cederlane,
138 Burlington, ON, dilution 1:500, collagen IV; mouse anti-human IgG, Dako, Carpinteria,
139 CA, dilution 1:50, and fibronectin; unconjugated rabbit polyclonal antibody, Biorbyt, San
140 Francisco, CA, dilution 1:150). The biotinylated secondary antibodies were applied at the
141 same concentrations as the primary antibodies for 45 minutes. Vectastain ABC kit
142 (Biolynx, Brockville, ON) was applied before DAB revelation (Vector Laboratories,
143 Peterborough, UK) and a counterstain with Harry's hematoxylin. Negative controls were
144 also prepared. They were stained with rabbit or mouse IgG instead of the primary
145 antibodies to reveal potential unspecific staining. Using the negative controls as a
146 benchmark, a semi-quantitative score was established for the basement membrane,
147 smooth muscle, blood vessel and lamina propria labeling as follows: Grade 0: Absence of
148 staining, Grade 1: Presence of staining. From this score, an average was established to
149 compare the labeling difference between native and decellularized bronchi.

150 ## Bronchi recellularization protocol

151 Decellularized bronchi were split in two and secured on a sterile support, then cut into
152 small pieces of a maximum of 1x1cm and rinsed in sterile PBS 1X. Tissues were then
153 placed in a 24-well plate (Costar, Washington, D.C.) and recellularized with the ASM
154 cells between P4 and P7 at a concentration of 158,000 cells/cm^2. One and a half
155 milliliters of medium were added to the culture under the same condition described
156 above. After a 48-hour incubation, allowing primary adhesion, 1 ml of the medium was
157 changed in each well. Then, the medium was changed every other day. Tissues were
158 maintained in culture, in the same well, between 48 hours and 41 days or transferred at 31
159 days to a 6-well plate (Celltreat, Pepperell, MA) for 10 more days. Samples were
160 collected at day 2, 7, 14, 21 and 31 without tissue transfer and at day 41 with and without
161 tissue transfer (Supplemental figure 1).

162 ## Assessment of recellularization efficiency

163 Tissues were fixed in 10% formalin, paraffin-embedded then sliced at 4.5 µm thickness
164 and stained using Movat Pentachrome histological staining protocol. The qualitative
165 assessment of recellularization was based on a visual examination of the recellularized
166 tissue sections under the optical microscope at 100 and 200 magnifications using the
167 Panoptiq software, as previously described.

168 An immunofluorescence staining of 5 fresh-frozen bronchi recellularized at day 41 was
169 performed for α-SMA. Tissues were incubated with the primary antibody for 2 hours at
170 37°C (α-SMA anti-mouse IgG2a, 1:250, Sigma Aldrich, St-Louis, MO). The fluorescent
171 secondary antibody (Goat anti-mouse IgG, 1:1000, Invitrogen, Carlsbad, CA) was

incubated for 1 hour at room temperature. An isotype control was used as a benchmark for positive staining. The slides were analyzed under Olympus Fluoview FV1000 confocal unit attached to the inverted Olympus IX81 microscope (Olympus Canada, Richmond Hill, ON, Canada) and compared to their replicate on a Movat Pentachrome staining to confirm the histological results.

For scan electron microscopy, the recellularized bronchi were fixed in 2.5% glutaraldehyde, washed and post-fixed in 1% aqueous osmium tetroxide solution, and dehydrated in increasing series of alcohol (70% to 100%). After dehydration, the samples were dried on the LEICA EM CPD 300 Critical Point Apparatus, mounted on carbon tape and gold-plated on the Emitech K550 Metalizing Apparatus, photo-documented on the LEO 435VP Scanning Electron Microscope at the Advanced Diagnostic Center by Image - CADI - Faculty of Veterinary Medicine and Animal Science - University of São Paulo.

Statistical analyses

The values are expressed as mean ± standard error of the means (SEM). Values of DNA and total protein quantification were analyzed by use of the paired student test (GraphPad Prism 7). Immunohistochemistry scores were analyzed by an exact chi-square test to compare the prevalence of positive staining against the status of the bronchi (native or decellularized) using SAS v.9.3. Values of $P \leq 0.05$ were considered significant.

190 # Results

191 ## Decellularization efficiency assessment

192 ### Histological assessment

193 Visual examination under the optical microscope at magnifications 100 and 200
194 confirmed the absence of cellular structures in decellularized matrices in comparison to
195 the native bronchi (Fig 1). The epithelial cell layer was totally removed. It also showed a
196 preserved bronchial architecture after the decellularization process with a maintenance of
197 the tissue organization and the contents in collagen and elastic fibers.

198 ### DNA quantification and electrophoresis

199 A decrease in DNA concentration was observed in decellularized bronchi. The mean
200 DNA concentration in the native bronchi was 2529 ng/mg of tissue ± 72.7 whereas it was
201 29.6 ng/mg of tissue ± 5.6 ($p < 0.0001$; Fig 2a) after decellularization. Agarose gel
202 electrophoresis revealed that the remaining double-stranded DNA fragment lengths in
203 decellularized bronchi was less than 100 bp (Supplemental figure 2).

204 ### Protein quantification

205 Although the difference in total protein concentrations in the native and decellularized
206 bronchi was significant ($p = 0.01$), the decline in these concentrations remained moderate,
207 to approximately 100 mg/ml (Fig 2b). The qualitative and semi-quantitative evaluation
208 revealed that collagen I and IV are not affected by the decellularization process. The

209 fibronectin while decreased, remained detectable in abundant amounts in the
210 decellularized extracellular matrix (Fig 3k-3l).

211 Recellularization assessment

212 Five different equine bronchi were recellularized with 3 primary ASM cell lines between
213 passages 3 and 7. Recellularizations from 48 hours to 7 days were modest or absent in all
214 cell-tissue combinations tested (n = 19). However, between days 14 and 21, the ASM
215 cells were detectable in tissue in 17 out of 19 replicates made during 7 different
216 recellularization trials.

217 At 31 days, ASM cells were observed in all recellularized tissues (n = 20). On 4 different
218 recellularization assays, the amount of ASM cells within the scaffold was maximum at 41
219 days. The ASM cells that repopulated the decellularized bronchi were first located on the
220 surface of the basement membrane or in the extracellular smooth muscle matrix (14
221 days). At day 21, ASM cells were present in the smooth muscle layer of the
222 decellularized bronchi and appeared to colonize it preferentially (Fig 4). This was
223 confirmed between 31 and 41 days, with abundant cells in the muscular extracellular
224 matrix and adjacent to the bronchial cartilage. However, some cells remained located
225 above the basement membrane. In two recellularization trials with 3 biological replicates,
226 the recellularization was improved at 41 days by transferring the tissue at day 31 in
227 another well for 10 additional days of culture before harvesting.

228 The immunofluorescent staining confirmed the expression of α-SMA by the cells present
229 in zones of abundant recellularization in the smooth muscle matrix (Fig 5).

230 On scanning electron microscopy analysis, recellularization was identified in most
231 samples on the tissue surface. On some parts of the ECM, where the resistance seamed
232 reduced, the cells penetrated the tissues, as it is shown, Fig 6.

233 Discussion

234 In this study, we developed a protocol to recellularize decellularized respiratory bronchi
235 with ASM cells. The results showed a preferential migration and colonization of the
236 muscular extracellular matrix by these cells. This phenomenon is, to the best of our
237 knowledge, reported for the first time in any species. The protocol presented herein will
238 enable the study of the phenotypic changes of ASM cells by an asthmatic ECM.

239 The initial aim of tissue engineering was to develop organs devoid of immunogenic
240 rejections for transplantation [14, 15]. It was then adopted in pharmacological and
241 oncological researches to identify the cellular response to drugs and in diseases [16-18],
242 as the cells' behavior was shown to vary depending on the 3D structures of the substrate
243 [6, 19]. Different organs, including lung tissues, have been decellularized and then
244 recellularized [20-23], mainly with stem cells [24, 25]. Recent studies have recellularized
245 horse lung tissues with equine dermal fibroblasts and canine yolk sac cells [26], and
246 mouse lungs with human and murine fibroblasts [27]. McClure et *al.* grafted a
247 decellularized skeletal muscle in the gastrocnemius and demonstrated a regeneration of
248 the graft with the presence of cells and neuromuscular junctions [28]. However, none of
249 the studies reported a preferential recellularization for specific cell types when seeded on
250 a heterogenous biological matrix.

251 To the best of knowledge, the present study is the first to attempt to recellularize airways
252 with primary airway smooth muscle cells. Different combinations of smooth muscle cells
253 lineages and matrices were studied and resulted in the colonization of the bronchial
254 smooth muscle matrix by the ASM cells. This preferential colonization likely involved
255 complex cellular mechanisms including integrin expression, adhesion, migration and
256 proliferation and suggests that the decellularized tissue retained enough of its native
257 qualities to allow this process to occur. Da Palma et *al.* demonstrated that the fibroblasts
258 recellularizing a decellularized horse lung are expressing the N-cadherin, an adhesion
259 biomarker [26]. This protein may play an important role in the ASM cell migration seen
260 in our study as it has been shown that the migration of the vascular smooth muscle cells is
261 delayed by the inhibition or the down-regulation of the N-cadherin [29, 30]. Moreover,
262 the ECM is known to regulate the migration of the ASM cells [31, 32].

263 The smooth muscle colonization was uneven as some parts of the bronchi contained more
264 ASM cells than other. This unevenness in cell distribution has also been observed during
265 lung recellularization by endothelial cells [33]. Uygun et *al.* also described variable
266 hepatocytes distribution within hepatic matrix [34]. This may be due to the uneven
267 mechanical properties of the decellularized bronchi as scan electron microscopy results
268 suggest that cells seem to reach the smooth muscle ECM from zones with low tissue
269 resistance.

270 The presence of matrikines in the scaffolds may also have contributed to this preferential
271 cell colonization. Matrikines are peptides produced from the proteolytic degradation of
272 the extracellular matrix [35]. Given the cellular destruction that occurs during
273 decellularization, the release of intracellular proteases may have resulted in the

274 production of a high concentration of matrikines within the scaffolds. These peptides
275 would affect cell behavior across integrins by stimulating the secretion of certain growth
276 factors. It has been shown that valine-glycine-proline-valine-glycine (VGPVG), a
277 hydrophobic elastin matrikine, stimulates smooth muscle cell proliferation [36]. The
278 tripeptide sequence Arginine-Phenylalanine-Lysine (RFK) derived from
279 thrombospondin-I is also mitogenic to smooth muscle cells through the activation of the
280 transforming growth factor (TGF)β [37]. Another peptide, valine-glycine-valine-arginine-
281 proline-glycine (VGVAPG), is chemotactic for fibroblasts [38]. These matrix fragments
282 being mobile and regulating cell behavior, would be potential promoters of myocyte
283 migration observed during recellularization.

284 GAGs are involved in different biological processes including extracellular matrix-cell
285 interaction and activation of various chemokines [39]. They are stained blue on histology
286 using Movat Pentachrome. Interestingly, from the 31st day of recellularization, a blue
287 coloration in the recellularized zones appeared on the Movat Pentachrome histological
288 staining in 4 of 20 bronchi studied. These findings suggest the secretion of GAGs by the
289 ASM cells, which are known to be secretory of these mucopolysaccharides [40].

290 No decellularization method is, to date, able to offer a complete elimination of the
291 cellular material [41]. Thus, four criteria are used to assess the quality of a decellularized
292 matrix: 1) maintenance of matrixial structural protein content, 2) absence of cellular
293 material on histological staining, 3) double stranded DNA should be less than 50 ng/mg
294 tissue and 4) less than 200 bp in length [42, 43]. In agreement with these reports, the
295 bronchial extracellular matrix was histologically free of cellular material with a global
296 maintenance of the bronchial architecture. The DNA concentrations we obtained by

297 fluorometry and electrophoresis were below the thresholds recommended to avoid in
298 vitro cytocompatibility problems [43]. However, in the context of regenerative medicine,
299 Allman et *al.* showed that the immunoreactivity of the remnant DNA in a transplanted
300 decellularized matrix could induce graft acceptance through a Th2 type response [44].

301 The decellularization protocol that was implemented herein was previously shown to
302 allow a better preservation of the extracellular matrix than other methods [11, 45]. The
303 total proteins fluorometric quantification revealed a significant concentration decrease of
304 matrixial proteins in the decellularized bronchi compared to the native ones. This
305 variation was expected as different intracellular proteins are eliminated during this
306 process but the effects on the matrixial proteins seem to depend on the nature of the
307 treated tissue [46, 47]. It has been shown that some cytoskeletal proteins, including α-
308 SMA and SMMHC, could be detected in decellularized matrices [11, 47, 48] and
309 correspond to the cellular residues observed by electron microscopy [48]. Our results are
310 in agreement with these findings as on confocal microscopy, our decellularized matrices
311 showed staining for α-SMA in some smooth muscle matrix areas. Moreover, the
312 decellularized bronchi maintained their general architecture and protein composition
313 almost unchanged in collagen I and IV, elastic fibers and fibronectin based on
314 histological evaluation and semi-quantitative immunohistochemical scoring of native and
315 decellularized bronchi. Those observations were in agreement with previous reports
316 assessing the maintenance of these matrixial proteins [11, 14, 45, 48, 49]. Collagens and
317 fibronectin are important for recellularization. Among other roles, fibronectin allow cell
318 adhesion to the ECM and collagens are needed for their infiltration into it [47]. Laminin

319 and other matrixial proteins also have cellular adhesion properties and may affect cell
320 behavior and phenotype [50].

321 To conclude, we obtained a decellularized bronchial ECM that was successfully, while
322 incompletely, recellularized with primary mature ASM cells over 41 days of culture. We
323 described a preferential colonization of the smooth muscle ECM by these cells. Other
324 investigations would be necessary to identify the factors and proteins that may be
325 implicated in the ASM cell-specific recellularization observed.

326 Acknowledgements

327 The authors thank Dr. Guy Beauchamp for the statistical analysis and the Respiratory
328 Health Network of Quebec (RHN) for the tissue bank creation.

329 Conflict of interest statement

330 On behalf of all authors, the corresponding author states that there is no conflict of
331 interest.

Funding

This project was funded by the Canadian institute of health research (CIHR) (JPL: Grant number PJT-148807) and supported by the faculty of superior and postdoctoral studies (FESP) scholarships (SBH).

Ethical approval

All applicable international, national, and/or institutional guidelines for the care and use of animals were followed. The experimental protocol was approved by the ethical committee of the University of Montreal number Rech-1578.

References

1. Gibson PG. What do non-eosinophilic asthma and airway remodelling tell us about persistent asthma? Thorax. 2007;62(12):1034-6.

2. Chetta A, Marangio E, Olivieri D. Inhaled steroids and airway remodelling in asthma. Acta Biomed. 2003;74(3):121-5.

3. Cukierman E, Pankov R, Stevens DR, Yamada KM. Taking cell-matrix adhesions to the third dimension. Science. 2001;294(5547):1708-12.

4. Baharvand H, Hashemi SM, Kazemi Ashtiani S, Farrokhi A. Differentiation of human embryonic stem cells into hepatocytes in 2D and 3D culture systems in vitro. Int J Dev Biol. 2006;50(7):645-52.

5. Htwe SS, Harrington H, Knox A, Rose F, Aylott J, Haycock JW, et al. Investigating NF-kappaB signaling in lung fibroblasts in 2D and 3D culture systems. Respir Res [Internet]. 2015 Dec 1 PMC4666055]; 16:[1-9 pp.]. Available from: https://www.ncbi.nlm.nih.gov/pubmed/26619903.

360 6. Duval K, Grover H, Han LH, Mou Y, Pegoraro AF, Fredberg J, et al. Modeling
361 Physiological Events in 2D vs. 3D Cell Culture. Physiology (Bethesda). 2017;32(4):266-
362 77.

363
364 7. Kapalczynska M, Kolenda T, Przybyla W, Zajaczkowska M, Teresiak A, Filas V,
365 et al. 2D and 3D cell cultures - a comparison of different types of cancer cell cultures.
366 Arch Med Sci. 2018;14(4):910-9.

367
368 8. Bullone M, Lavoie JP. The equine asthma model of airway remodeling: from a
369 veterinary to a human perspective. Cell Tissue Res [Internet]. 2019 Nov 12. Available
370 from: https://www.ncbi.nlm.nih.gov/pubmed/31713728.

371
372 9. Herszberg B, Ramos-Barbon D, Tamaoka M, Martin JG, Lavoie JP. Heaves, an
373 asthma-like equine disease, involves airway smooth muscle remodeling. J Allergy Clin
374 Immunol. 2006;118(2):382-8.

375
376 10. Leclere M, Lavoie-Lamoureux A, Joubert P, Relave F, Setlakwe EL, Beauchamp
377 G, et al. Corticosteroids and antigen avoidance decrease airway smooth muscle mass in
378 an equine asthma model. Am J Respir Cell Mol Biol. 2012;47(5):589-96.

379
380 11. Wagner DE, Bonenfant NR, Sokocevic D, DeSarno MJ, Borg ZD, Parsons CS, et
381 al. Three-dimensional scaffolds of acellular human and porcine lungs for high throughput
382 studies of lung disease and regeneration. Biomaterials. 2014;35(9):2664-79.

383
384 12. Vargas A, Peltier A, Dube J, Lefebvre-Lavoie J, Moulin V, Goulet F, et al.
385 Evaluation of contractile phenotype in airway smooth muscle cells isolated from
386 endobronchial biopsy and tissue specimens from horses. Am J Vet Res. 2017;78(3):359-
387 70.

388
389 13. Russell HK, Jr. A modification of Movat's pentachrome stain. Arch Pathol.
390 1972;94(2):187-91.

391
392 14. Baiguera S, Del Gaudio C, Jaus MO, Polizzi L, Gonfiotti A, Comin CE, et al.
393 Long-term changes to in vitro preserved bioengineered human trachea and their
394 implications for decellularized tissues. Biomaterials. 2012;33(14):3662-72.

395
396 15. Maghsoudlou P, Georgiades F, Tyraskis A, Totonelli G, Loukogeorgakis SP,
397 Orlando G, et al. Preservation of micro-architecture and angiogenic potential in a
398 pulmonary acellular matrix obtained using intermittent intra-tracheal flow of detergent
399 enzymatic treatment. Biomaterials. 2013;34(28):6638-48.

400

401 16. Langhans SA. Three-Dimensional in Vitro Cell Culture Models in Drug
402 Discovery and Drug Repositioning. Front Pharmacol [Internet]. 2018 PMC5787088]; 9:[6
403 p.]. Available from: https://www.ncbi.nlm.nih.gov/pubmed/29410625.

404

405 17. Yamada KM, Cukierman E. Modeling tissue morphogenesis and cancer in 3D.
406 Cell. 2007;130(4):601-10.

407

408 18. Fisher SA, Tam RY, Fokina A, Mahmoodi MM, Distefano MD, Shoichet MS.
409 Photo-immobilized EGF chemical gradients differentially impact breast cancer cell
410 invasion and drug response in defined 3D hydrogels. Biomaterials. 2018;178:751-66.

411

412 19. Edmondson R, Broglie JJ, Adcock AF, Yang L. Three-dimensional cell culture
413 systems and their applications in drug discovery and cell-based biosensors. Assay and
414 drug development technologies. 2014;12(4):207-18.

415

416 20. Totonelli G, Maghsoudlou P, Garriboli M, Riegler J, Orlando G, Burns AJ, et al.
417 A rat decellularized small bowel scaffold that preserves villus-crypt architecture for
418 intestinal regeneration. Biomaterials. 2012;33(12):3401-10.

419

420 21. Taylor DA, Sampaio LC, Cabello R, Elgalad A, Parikh R, Wood RP, et al.
421 Decellularization of Whole Human Heart Inside a Pressurized Pouch in an Inverted
422 Orientation. J Vis Exp [Internet]. 2018 Nov 26; (141). Available from:
423 https://www.ncbi.nlm.nih.gov/pubmed/30531712.

424

425 22. Xue A, Niu G, Chen Y, Li K, Xiao Z, Luan Y, et al. Recellularization of well-
426 preserved decellularized kidney scaffold using adipose tissue-derived stem cells. J
427 Biomed Mater Res A. 2018;106(3):805-14.

428

429 23. Stahl EC, Bonvillain RW, Skillen CD, Burger BL, Hara H, Lee W, et al.
430 Evaluation of the host immune response to decellularized lung scaffolds derived from
431 alpha-Gal knockout pigs in a non-human primate model. Biomaterials. 2018;187:93-104.

432

433 24. Crabbe A, Liu Y, Sarker SF, Bonenfant NR, Barrila J, Borg ZD, et al.
434 Recellularization of decellularized lung scaffolds is enhanced by dynamic suspension
435 culture. PLoS One [Internet]. 2015 PMC4427280]; 10(5):[e0126846 p.]. Available from:
436 https://www.ncbi.nlm.nih.gov/pubmed/25962111.

437

438 25. Doi R, Tsuchiya T, Mitsutake N, Nishimura S, Matsuu-Matsuyama M, Nakazawa
439 Y, et al. Transplantation of bioengineered rat lungs recellularized with endothelial and
440 adipose-derived stromal cells. Sci Rep [Internet]. 2017 Aug 16 PMC5559597];
441 7(1):[8447 p.]. Available from: https://www.ncbi.nlm.nih.gov/pubmed/28814761.

442
443 26. da Palma RK, Fratini P, Schiavo Matias GS, Cereta AD, Guimaraes LL,
444 Anunciacao ARA, et al. Equine lung decellularization: a potential approach for in vitro
445 modeling the role of the extracellular matrix in asthma. J Tissue Eng. 2018;9:1-11.

446
447 27. Burgstaller G, Sengupta A, Vierkotten S, Preissler G, Lindner M, Behr J, et al.
448 Distinct niches within the extracellular matrix dictate fibroblast function in (cell free) 3D
449 lung tissue cultures. Am J Physiol Lung Cell Mol Physiol. 2018;314(5):708-23.

450
451 28. McClure MJ, Cohen DJ, Ramey AN, Bivens CB, Mallu S, Isaacs JE, et al.
452 Decellularized muscle supports new muscle fibers and improves function following
453 volumetric injury. Tissue Eng Part A. 2018;24(15-16):1228-41.

454
455 29. Lyon CA, Koutsouki E, Aguilera CM, Blaschuk OW, George SJ. Inhibition of N-
456 cadherin retards smooth muscle cell migration and intimal thickening via induction of
457 apoptosis. J Vasc Surg. 2010;52(5):1301-9.

458
459 30. Wang X, Du C, He X, Deng X, He Y, Zhou X. MiR-4463 inhibits the migration
460 of human aortic smooth muscle cells by AMOT. Biosci Rep [Internet]. 2018 Oct 31
461 PMC6147913]; 38(5). Available from: https://www.ncbi.nlm.nih.gov/pubmed/29752344.

462
463 31. Parameswaran K, Radford K, Zuo J, Janssen LJ, O'Byrne PM, Cox PG.
464 Extracellular matrix regulates human airway smooth muscle cell migration. Eur Respir J.
465 2004;24(4):545-51.

466
467 32. Madison JM. Migration of airway smooth muscle cells. Am J Respir Cell Mol
468 Biol. 2003;29(1):8-11.

469
470 33. Scarritt ME, Pashos NC, Motherwell JM, Eagle ZR, Burkett BJ, Gregory AN, et
471 al. Re-endothelialization of rat lung scaffolds through passive, gravity-driven seeding of
472 segment-specific pulmonary endothelial cells. J Tissue Eng Regen Med. 2018;12(2):786-
473 806.

474
475 34. Uygun BE, Yarmush ML, Uygun K. Application of whole-organ tissue
476 engineering in hepatology. Nat Rev Gastroenterol Hepatol. 2012;9(12):738-44.

477
478 35. La Rocca G, Anzalone R, Magno F, Corrao S, Carbone M, Loria L, et al. New
479 perspectives on the roles of proteinases and lung structural cells in the pathogenesis of
480 chronic obstructive pulmonary disease. In: Gerbino A, Zummo G, Crescimanno G,
481 editors. Experimental medicine reviews Plumelia Ricerca ed2007. p. 328.

482

483 36. Wachi H, Seyama Y, Yamashita S, Suganami H, Uemura Y, Okamoto K, et al.
484 Stimulation of cell proliferation and autoregulation of elastin expression by elastin
485 peptide VPGVG in cultured chick vascular smooth muscle cells. FEBS Lett.
486 1995;368(2):215-9.

487

488 37. Ribeiro SM, Poczatek M, Schultz-Cherry S, Villain M, Murphy-Ullrich JE. The
489 activation sequence of thrombospondin-1 interacts with the latency-associated peptide to
490 regulate activation of latent transforming growth factor-beta. The Journal of biological
491 chemistry. 1999;274(19):13586-93.

492

493 38. Senior RM, Griffin GL, Mecham RP, Wrenn DS, Prasad KU, Urry DW. Val-Gly-
494 Val-Ala-Pro-Gly, a repeating peptide in elastin, is chemotactic for fibroblasts and
495 monocytes. J Cell Biol. 1984;99(3):870-4.

496

497 39. Papakonstantinou E, Karakiulakis G. The 'sweet' and 'bitter' involvement of
498 glycosaminoglycans in lung diseases: pharmacotherapeutic relevance. Br J Pharmacol.
499 2009;157(7):1111-27.

500

501 40. Nigro J, Wang A, Mukhopadhyay D, Lauer M, Midura RJ, Sackstein R, et al.
502 Regulation of heparan sulfate and chondroitin sulfate glycosaminoglycan biosynthesis by
503 4-fluoro-glucosamine in murine airway smooth muscle cells. The Journal of biological
504 chemistry. 2009;284(25):16832-9.

505

506 41. Gilbert TW, Freund JM, Badylak SF. Quantification of DNA biologic scaffold
507 materials. The journal of surgical research. 2009;1(152):135-9.

508

509 42. Gilpin A, Yang Y. Decellularization Strategies for Regenerative Medicine: From
510 Processing Techniques to Applications. Biomed Res Int [Internet]. 2017 PMC5429943];
511 2017:[9831534 p.]. Available from: https://www.ncbi.nlm.nih.gov/pubmed/28540307.

512

513 43. Crapo PM, Gilbert TW, Badylak SF. An overview of tissue and whole organ
514 decellularization processes. Biomaterials. 2011;32(12):3233-43.

515

516 44. Allman AJ, McPherson TB, Badylak SF, Merrill LC, Kallakury B, Sheehan C, et
517 al. Xenogeneic extracellular matrix grafts elicit a TH2-restricted immune response.
518 Transplantation. 2001;71(11):1631-40.

519

520 45. Tsuchiya T, Sivarapatna A, Rocco K, Nanashima A, Nagayasu T, Niklason LE.
521 Future prospects for tissue engineered lung transplantation: decellularization and
522 recellularization-based whole lung regeneration. Organogenesis. 2014;10(2):196-207.

523

524 46. Grauss RW, Hazekamp MG, Oppenhuizen F, van Munsteren CJ, Gittenberger-de
525 Groot AC, DeRuiter MC. Histological evaluation of decellularised porcine aortic valves:
526 matrix changes due to different decellularisation methods. Eur J Cardiothorac Surg.
527 2005;27(4):566-71.

528

529 47. Gilbert TW, Sellaro TL, Badylak SF. Decellularization of tissues and organs.
530 Biomaterials. 2006;27(19):3675-83.

531

532 48. Bonvillain RW, Danchuk S, Sullivan DE, Betancourt AM, Semon JA, Eagle ME,
533 et al. A nonhuman primate model of lung regeneration: detergent-mediated
534 decellularization and initial in vitro recellularization with mesenchymal stem cells. Tissue
535 Eng Part A. 2012;18(23-24):2437-52.

536

537 49. Chani B, Puri V, Sobti RC, Jha V, Puri S. Decellularized scaffold of
538 cryopreserved rat kidney retains its recellularization potential. PLos One [Internet]. 2017
539 PMC5340383]; 12(3). Available from: https://www.ncbi.nlm.nih.gov/pubmed/28267813.

540

541 50. Halper J, Kjaer M. Basic components of connective tissues and extracellular
542 matrix: elastin, fibrillin, fibulins, fibrinogen, fibronectin, laminin, tenascins and
543 thrombospondins. Adv Exp Med Biol. 2014;802:31-47.

544

545

546 # Figures and supplemental Figures legends

547 **Fig 1. Movat Pentachrome staining of a native and a decellularized bronchus at**
548 **magnification 100.** (a) native bronchus, (b) decellularized bronchus. From top to bottom,
549 on each image, the bronchial cartilage, followed by the bronchial smooth muscle
550 surrounded on both sides by the extracellular matrix which, at the level of the lamina
551 propria, is followed by the epithelial cells layer. Collagen is stained in yellow. The black
552 filamentous structures on (a) and on (b) represent the elastic fibers. The cell nuclei are
553 stained in purple, their omnipresence is noted on (a) and their total absence on (b). Scale
554 bars indicate 100 µm.

555 **Fig 2. DNA and total protein concentrations in native and decellularizd bronchi.** (a)
556 DNA concentration in ng/mg of tissue in 7 native and decellularized bronchi, (b) Total
557 protein concentration in mg/ml in 7 native and decellularized bronchi. A significant
558 difference is found for DNA and total protein concentrations between native and
559 decellularized bronchi with respectively, $p < 0.0001$ and $p = 0.01$.

560 **Fig 3. Immunohistochemical staining for Collagen I and IV and for fibronectin in**
561 **native and decellularized bronchi at magnification 100.** Native and decellularized
562 bronchi stained for collagen I (a, b, c, d), collagen IV (e, f, g, h) and fibronectin (i, j, k, l).
563 Evaluation of positive staining (c, d, g, h, k, l) compared to isotypic controls (a, b, e, f, i,
564 j). Scale bars indicate 100 µm.

565 **Fig 4. Movat Pentachrome staining at magnification 100 showing the**
566 **recellularization between day 0 and day 41.** The ASM cell nuclei are stained in purple.
567 (a) decellularized bronchi on day 0; (b) recellularized bronchi on day 14 with ASM cells

568 at the surface and in the collagenous ECM of the smooth muscle; (c) recellularized
569 bronchi on day 21 with ASM cells more organized at the level of the smooth muscle
570 ECM and lined with bronchial cartilage; (d) recellularized bronchi on day 41 with
571 confluent ASM cells in the smooth muscle extracellular matrix and on the surface of the
572 basement membrane. Scale bars indicate 100 µm.

573 **Fig 5. Movat Pentachrome and α-SMA immunofluorescence consecutive staining of**
574 **recellularized bronchial matrix at day 41.** (a) and (b): Movat Pentachrome and
575 immunofluorescence staining of the same area in a recellularized bronchus at
576 magnification 100. (c) and (d): Movat Pentachrome and immunofluorescence staining of
577 the same area in a recellularized bronchus at magnification 400. The cells recellularizing
578 the tissue are expressing the α-SMA which is an indication of the smooth muscle nature
579 of the cells colonizing the tissue and their purity. Scale bars are indicating 100 µm for (a)
580 and (b) and 25 µm for (c) and (d).

581 **Fig 6. Scan electron microscopy of decellularized and 41 days recellularized**
582 **bronchial matrices.** (a) decellularized matrix; (b) recellularized matrix with cells
583 appearing on the surface; (c) cross section of recellularized matrix, cells are only on the
584 surface but not inside the tissue; (d) cross section of recellularized matrix, cells are
585 penetrating the tissue. The red arrows are indicating some of the cells. Scale bars are
586 indicating 3 µm for (a) and (b) and 30 µm for (c) and (d).

587 **S1 Fig. Time chart of the recellularizations.** R is indicating recellularization at day 0
588 and S is referring to sampling on the timeline.

589 **S2 Fig. DNA electrophoresis for native and decellularized bronchi.** The abbreviation

590 N.Br is for native bronchi and D.Br for decellularized ones.

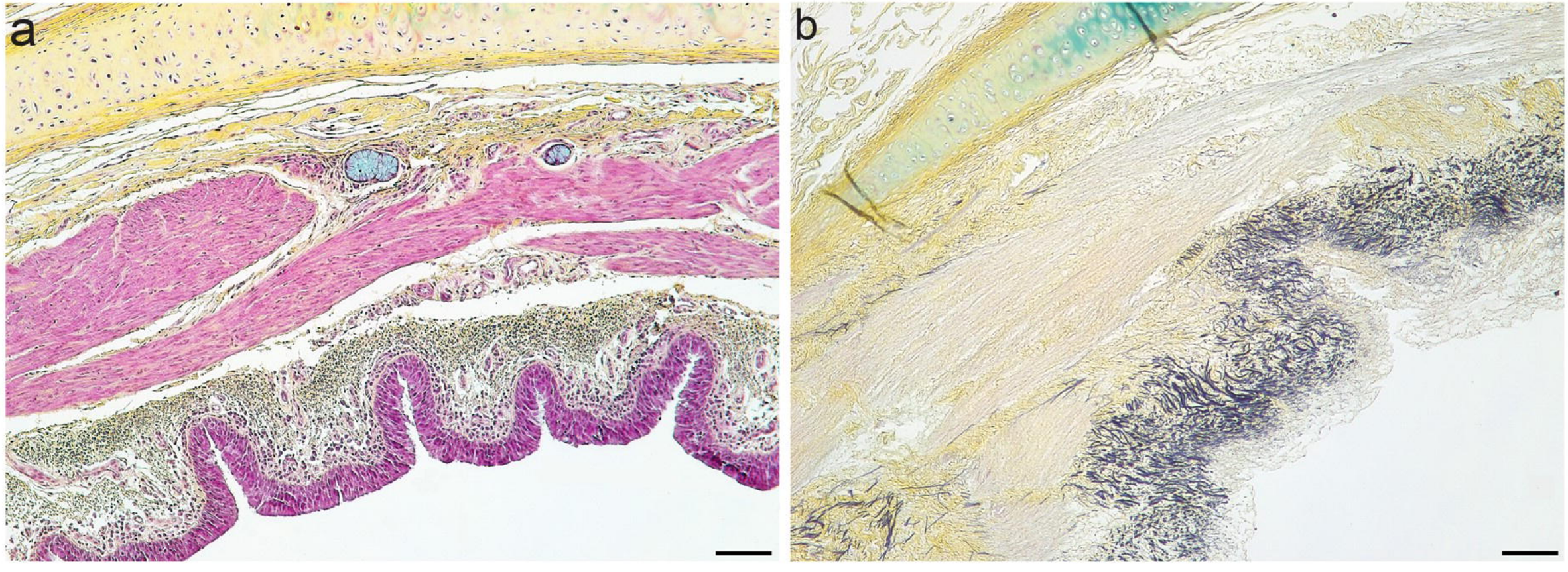
a
b

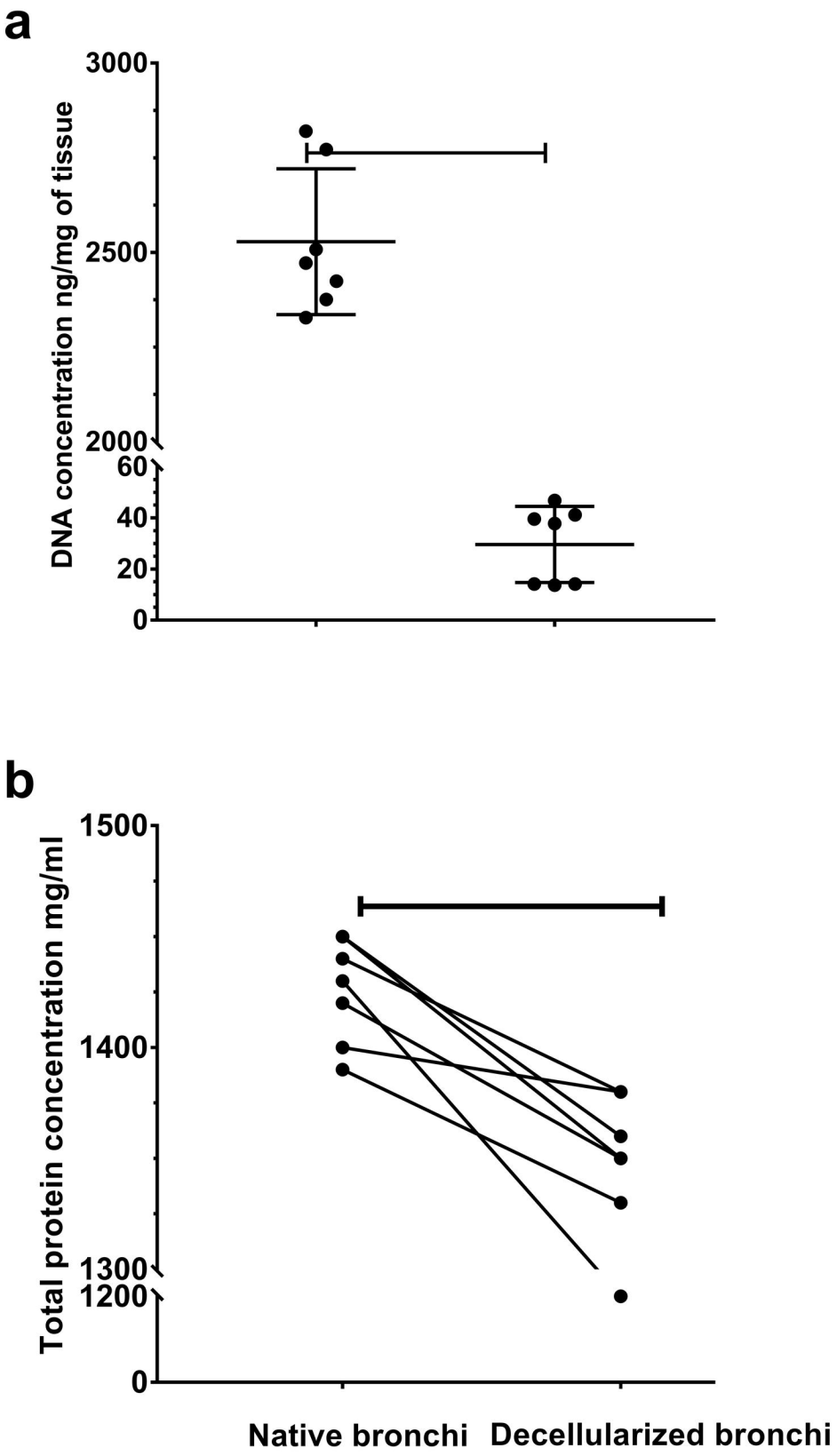
a
DNA concentration ng/mg of tissue
3000
2500
2000
60
40
20
0
b
Total protein concentration mg/ml
1500
1400
1300
1200
0
Native bronchi
Decellularized bronchi

Collagen I
Collagen IV
Fibronectin
a
b
c
d
e
f
g
h
i
j
k
l

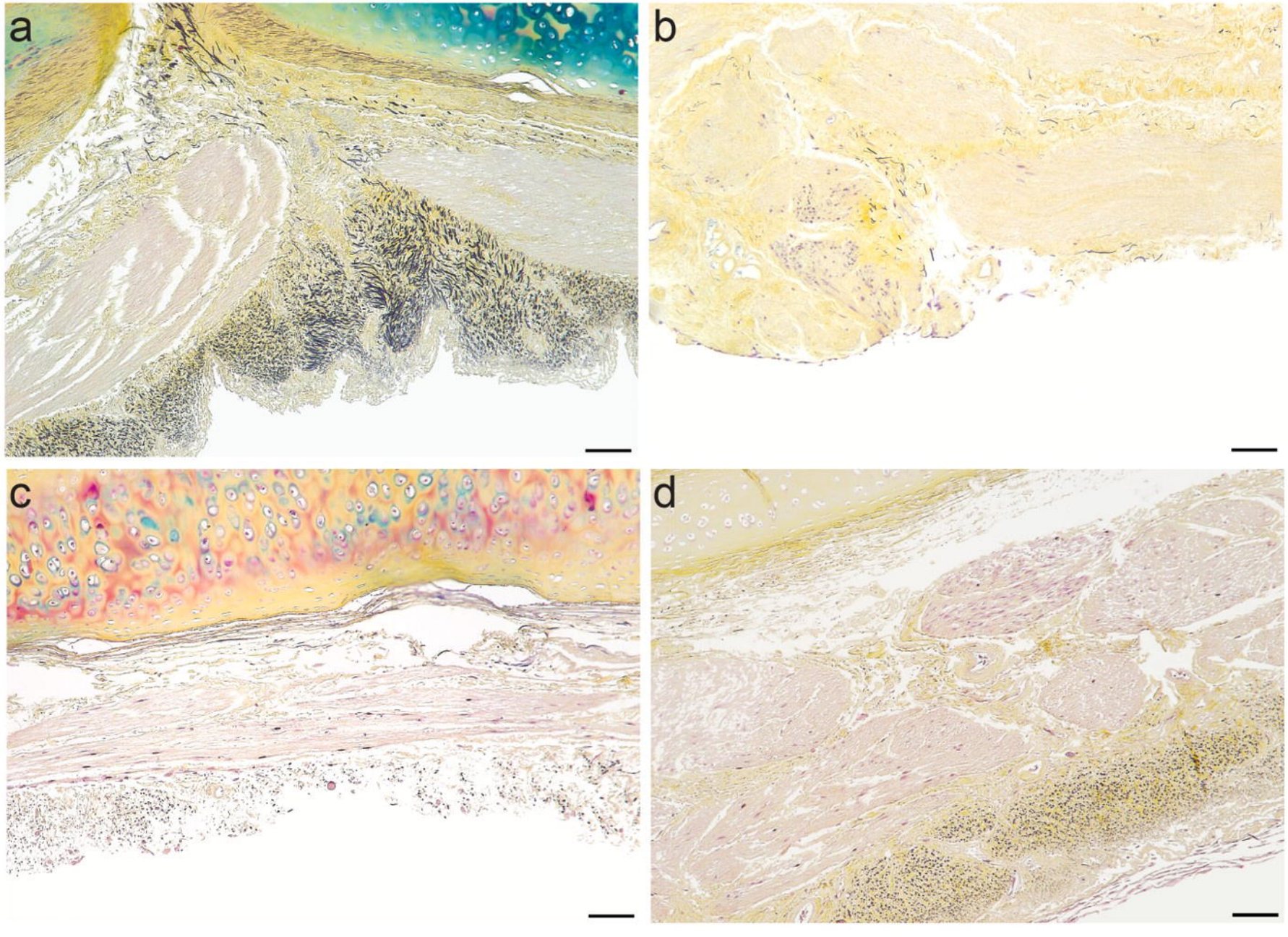
a
b
c
d

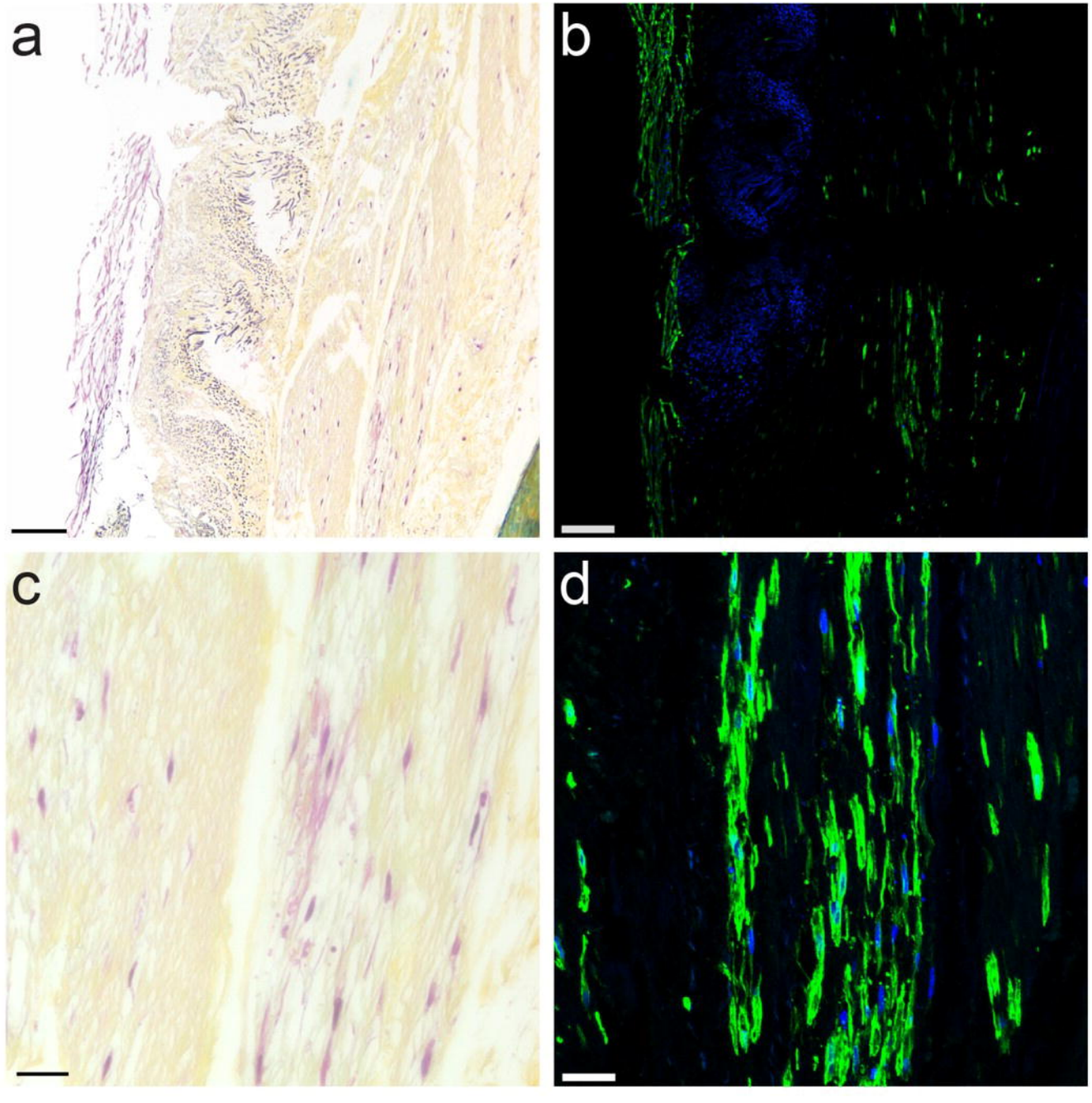
a
b
c
d

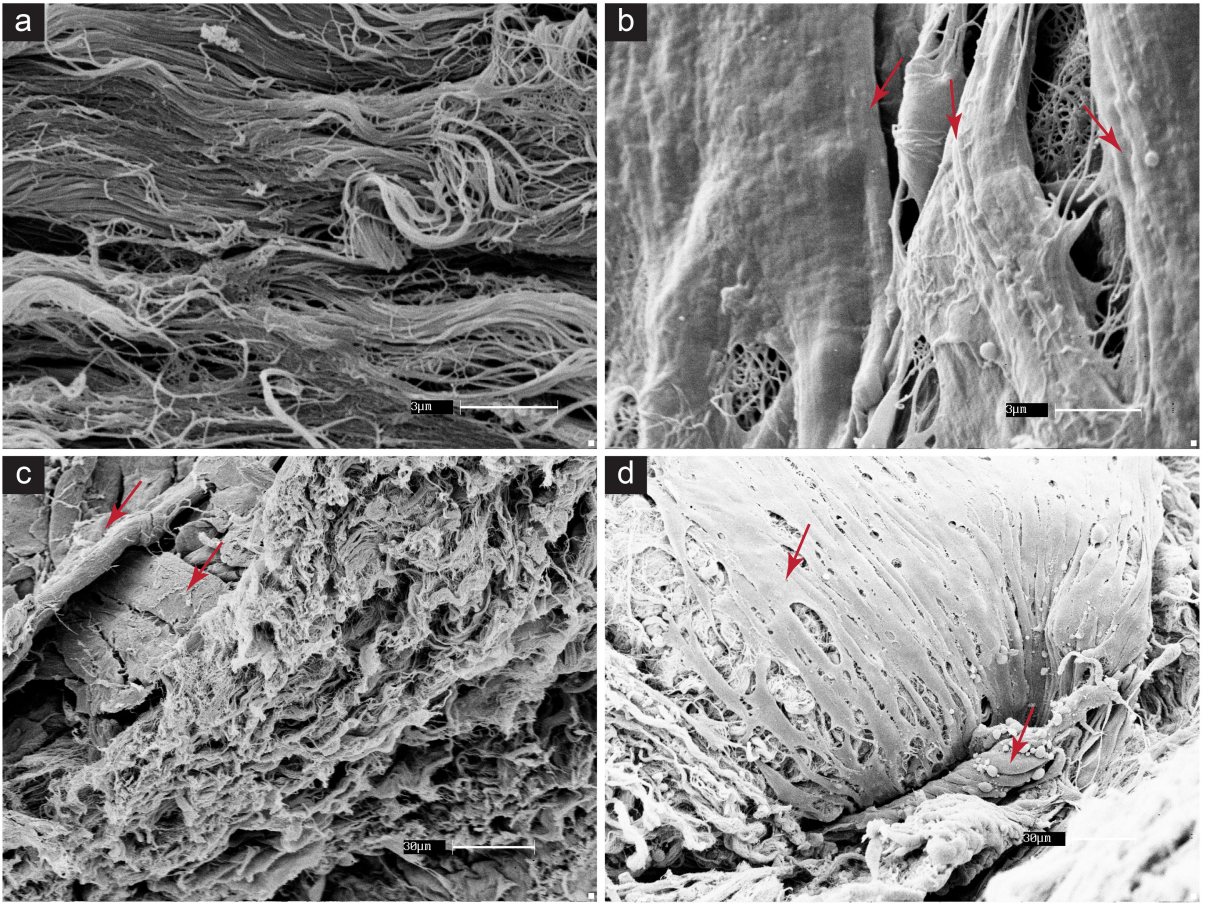
a
3μm
b
3μm
c
30μm
d
30μm